

Estimating abundance from gillnet samples with application to red drum (*Sciaenops ocellatus*) in Texas bays

Clay E. Porch, Mark R. Fisher, and Lawrence W. McEachron

Abstract: A model of gillnet selection is developed to accommodate the possibility that some catch observations will be known more precisely than others and allow for nonlinear relationships between the selection parameters and mesh size. The model is used to show that gillnet selection for red drum (*Sciaenops ocellatus*) in Texas bays may be explained as a unimodal process approximating a skewed Laplace distribution, where the optimal length varies in proportion to mesh size and the variance in proportion to the optimal length. It is also suggested that the number of encounters with the net ought to depend on swimming speed of the quarry, which in turn varies predictably with length. This information, along with the estimates of selection, is used to develop indices of abundance for each length-class. The results indicate that the recruitment of year-old red drum to Texas bays has fluctuated markedly since 1975, but without any persistent trends. However, the survival of these and older fish has increased dramatically owing to various regulations promulgated since 1981.

Résumé : Un nouveau modèle de sélection des filets maillants permet de tenir compte de la possibilité que certaines observations de captures soient plus précises que d'autres et qu'il y ait des relations non-linéaires entre les paramètres de sélection et la dimension de la maille du filet. Le modèle est utilisé pour démontrer que la sélection exercée par les filets maillants sur le tambour rouge (*Sciaenops ocellatus*) des baies du Texas s'explique comme un processus unimodal s'approchant d'une distribution de Laplace asymétrique dans laquelle la logueur optimale varie en proportion de la dimension de la maille et la variance, en fonction de la longueur optimale. Nous avançons aussi l'hypothèse que le nombre de rencontres avec le filet dépend de la vitesse de nage de la proie, qui est, elle-même, fonction de sa longueur. Ces renseignements, ajoutés aux estimations de sélection, nous ont permis de calculer des indices d'abondance pour chaque classe de longueur. Il en ressort que le recrutement des tambours rouges de 1 an dans les baies du Texas a fluctué de façon importante depuis 1975, mais sans tendance bien marquée. Néanmoins, la survie de ces poissons et celle des poissons plus âgés a augmenté de façon spectaculaire à cause de diverses réglementations en vigueur depuis 1981.

[Traduit par la Rédaction]

Introduction

Gillnets are widely used to monitor the abundance of fish populations, but are highly selective. As a result, the length structure of the catch may differ substantially from that of the sampled population. This difference is usually corrected for by dividing the catch of each length-class with an estimate of the net's selectivity towards that length-class. If the length structure of the population is known for some portion of the time series, then the estimation of selection is straightforward (catch divided by abundance). Otherwise, selection can be estimated indirectly from the length–frequency distri-

butions of several different mesh sizes fished simultaneously.

Most “indirect” methods operate by fitting selection curves to the length–frequency distributions of each mesh size or the mesh frequency distributions of each length-class. The earliest applications assumed that the shape of the selection curve was the same for all mesh sizes. Helser et al. (1991) and Hovgard (1996) have since developed numerical methods that relax this assumption somewhat, but the former still requires the height of the selection curve to be the same for all mesh sizes and the latter requires the variance of the selection curve to be proportional to the square of the mesh size (essentially implying a constant coefficient of variation). Both methods also assume that the most vulnerable length-class (optimal length) is a linear function of mesh size.

Another important limitation of existing indirect methods is that they are conditioned on the number of fish that actually encounter the net, which means that the selection estimates reflect the proportion of fish captured from the encountered population rather than from the population as a whole. Thus, if the desire is to construct indices of abundance, account must be taken of factors that may cause the number of encounters to differ from the number of animals in the population.

The purpose of this paper is to present a generalized

Received 1 February 2001. Accepted 27 March 2002.

Published on the NRC Research Press Web site at

<http://cjfas.nrc.ca> on 11 May 2002.

J16202

C.E. Porch.¹ Southeast Fisheries Science Center, Sustainable Fisheries Division, NOAA Fisheries, 75 Virginia Beach Drive, Miami, FL 33149, U.S.A.

M.R. Fisher and L.W. McEachron.² Texas Parks and Wildlife, Coastal Fisheries Division, 4200 Smith School Road, Austin, TX 78744, U.S.A.

¹Corresponding author (e-mail: clay.porch@noaa.gov).

²Deceased.

method for estimating selection and population abundance from gillnet catches. The proposed methodology builds on the least-squares approach of Hovgard (1996) by accommodating nonlinear relationships between the selection parameters and mesh size as well as variations in selection over time and space. The least-squares estimation procedure is also extended to allow for the fact that some catch observations are known more precisely than others. Finally, the encounter rate is modeled as a function of the swimming speed of the quarry, which provides a means for converting estimates of the number of encounters to estimates of abundance. The proposed models are applied to catch-at-length observations from red drum (*Sciaenops ocellatus*) collected during gillnet surveys conducted in Texas bays.

Materials and methods

Selection model

The expected number of fish caught (C) by a gillnet may be expressed as a function of effort (f), fishing power (p), selection (S), and encounters per unit effort (E)

$$(1) \quad C_{mkl} = f_{mk} p_{mk} S_{mkl} E_{kl}$$

where the subscripts m , l , and k refer to mesh size, length, and stratum (e.g., time or area). In this notation, p is the probability of capture for the length-class that is most vulnerable upon encountering the net and S gives the probability of capture for each length-class relative to p . Together they dictate the height and shape of the S curve.

The system described in eq. 1 has more unknowns than equations, making it necessary to impose some additional structure. Most methods accomplish this by assuming that p is the same for all m and requiring S to be of a particular functional form. However, the assumption that p is the same for all m is generally untrue and can lead to substantial bias (Hamley 1975). Moreover, p may be expected to vary in space and time. Fortunately, the need to assume a constant p arose principally as a matter of algebraic convenience and is unnecessary in numerical schemes. Unique solutions to the system in eq. 1 can be shown to exist whenever two fairly liberal conditions are met: (i) the p value for each mesh is constant over several, but not necessarily all, k and (ii) the shape of S can be described by a mathematical function with reasonably few parameters compared with the number of l categories. In practice, the estimates for the absolute magnitude of the p s will be poorly determined unless there is considerable contrast in the data. Therefore it will usually be prudent to fix the value of p for one of the m to an arbitrary standard (say 1.0) over several k . The estimates of E and p for the remaining k must be regarded as relative values, but this should be of little consequence inasmuch as the "absolute" values themselves typically represent an unknown fraction of the population that is available to the gear.

Several mathematical functions have been used to model the curve S to the satisfaction of condition (ii) above, including the normal, lognormal, gamma, and Pearson type 1 curves. Another potential candidate is the Laplace curve, which can accommodate narrower peaks and thicker tails than the others. The equations for these curves may all be expressed in terms of the size of most vulnerable length-class (optimal l) λ and variance in length, σ^2 (see Table 1).

However, the model's ability to produce precise estimates may be enhanced if λ and σ^2 can be expressed as a function of m .

Most researchers have adopted Baranov's similarity principle and assumed that λ is proportional to m and that σ^2 is constant. Regier and Robson (1966) and Hovgard (1996), however, allowed σ^2 to be proportional to m^2 . In point of fact, it is quite possible that λ and σ^2 are both nonlinearly related to m owing to asymmetries in growth, net elasticity, and other factors. Therefore, it is useful to express them as more general functions of, such as the power functions $\lambda = \alpha m^\beta$ and $\sigma^2 = \gamma \lambda^\delta$. Similarly, additional skew may be admitted by use of the Gram-Charlier series (Table 1), where the skew parameter θ can be expressed as the quadratic $\theta = \theta_1 + \theta_2 m + \theta_3 m^2$ rather than a power function to allow for changes in sign (Helser et al. 1991).

Parameter estimation

The selection model in system (1) has now been reduced to a function of p , optimal length (α and β), variance (γ and δ), and skewness (θ_1 , θ_2 , θ_3). In principle, all of these parameters may be estimated by minimizing an objective function involving one of the S curves in Table 1, provided of course they are each invariant over some subset of k . Hovgard (1996) advocated the use of least squares, which implies an additive error with constant variance. It is likely, however, that the variance in catch-at-length will increase with larger catches or fewer samples. Accordingly, we adopted a weighted least-squares (\mathcal{Q}) procedure that minimizes

$$(2) \quad \mathcal{Q} = \sum_l \sum_k \sum_m \frac{(C_{mkl} - f_{mk} p_{mk} S_{mkl} E_{kl})^2}{2V\{C_{mkl}\}}$$

where V denotes the variance of the catch-at-length observation (see Appendix A).

A practical difficulty with applying eq. 2 is that the number of E parameters will often be very large (there are 8421 in the red drum example below) and the search time for optimization algorithms increases geometrically with the number of parameters. However, as Hovgard (1996) pointed out for ordinary least squares, analytical expressions for E may be obtained by setting the derivatives of eq. 2 equal to zero and solving with respect to E , p and S being regarded as constant

$$(3) \quad E_{kl} = \frac{\sum_m C_{mkl} f_{mk} p_{mk} S_{mkl} / V\{C_{mkl}\}}{\sum_m f_{mk}^2 p_{mk}^2 S_{mkl}^2 / V\{C_{mkl}\}}$$

Substituting eq. 3 into eq. 2 produces an objective function with the same minimum as the original problem (Seber and Wild 1989). Covariances and percentile confidence limits for the p , S , and E parameters were derived by use of a parametric bootstrap (see Appendix B).

Model building

Akaike's information criteria for small samples (AIC_c) was used to determine the combination of selection parameters and type of S curve that provided the most parsimonious explanation of the data (Hurvich and Tsai 1995; Buckland et

Table 1. Mathematical functions used to model selection (*S*).

Function name	Mathematical representation	Comments
Normal	$\frac{1}{\sqrt{2\pi\sigma^2}} e^{-0.5(l-\lambda)^2/\sigma^2}$	Most common choice in the literature (e.g., Baranov 1948; Holt 1963)
Laplace (double exponential)	$\frac{1}{\sqrt{2}\sigma} e^{-\sqrt{2} l-\lambda /\sigma}$	Similar to normal curve, but with thicker tails
Lognormal	$\frac{1}{\sqrt{2\pi\sigma^2}l} e^{-0.5(\log_e[l]-\log_e[\lambda])^2/\sigma^2}$	Asymmetric curve used by McCombie and Fry (1960)
Gamma	$\frac{1}{\Gamma(A)} B^{-A} l^{A-1} e^{-l/B}$	Asymmetric curve used by Regier and Robson (1966) (Note: $A = (\lambda/\sigma)^2$ and $B = \sigma^2/\lambda$)
Pearson type 1	$\left(1.0 + \frac{l-\lambda}{b}\right)^{bd} \left(1.0 + \frac{l-\lambda}{c}\right)^{cd}$	Asymmetric curve (Hamley and Regier 1973) (Note: b and c are distance to the right and left of λ where $S = 0$; d determines kurtosis)
Gram-Charlier series	$1.0 - 0.5\theta\sigma^{3/2} \left(\frac{(l-\lambda)}{\sigma} - \frac{(l-\lambda)^3}{3\sigma^3}\right)$	A multiplicative factor used to skew other functions (see Croxton et al. 1967; McCombie and Berst 1969)

Note: The variables λ and σ refer to the optimal length and standard deviation in length, respectively. In practice, the equations are discretized by allowing l to represent the midpoint of each length-class and dividing by the sum over all length-classes.

Table 2. Number of gillnet sets by fishing year and bay system.

Fishing year	Sabine Lake	Galveston	Matagorda	San Antonio	Aransas	Corpus Christi	Upper Laguna Madre	Lower Laguna Madre	East Matagorda	Total
1975	2	12	7	7	7	7	8	7	0	57
1976	0	20	14	14	14	14	14	14	8	112
1977	0	16	16	16	16	16	16	16	16	128
1978	0	20	20	20	20	20	20	20	20	160
1979	0	32	32	32	32	32	32	32	24	248
1980	0	20	20	20	20	20	20	20	20	160
1981	0	90	90	90	90	90	90	90	16	646
1982	0	90	90	90	90	90	90	90	20	650
1983	0	90	90	90	90	90	90	90	20	650
1984	0	90	90	90	90	90	90	90	40	670
1985	45	90	90	90	90	90	90	90	40	715
1986	90	90	90	90	90	90	90	90	40	760
1987	90	90	90	90	90	90	90	90	40	760
1988	90	90	90	90	90	90	90	90	40	760
1989	90	90	90	90	90	90	90	90	40	760
1990	90	90	90	90	90	90	90	90	40	760
1991	90	90	90	90	90	90	90	90	40	760
1992	90	90	90	90	90	90	90	90	40	760
1993	90	90	90	90	90	90	90	90	40	760
1994	90	90	90	90	90	90	90	90	40	760
1995	90	90	90	90	90	90	90	90	40	760
1996	90	90	90	90	90	90	90	90	40	760
1997	90	90	90	90	90	90	90	90	40	760
1998	45	45	45	45	45	45	45	45	20	380
Total	1172	1695	1684	1684	1684	1684	1685	1684	724	13 696

al. 1997). Essentially, this amounted to minimizing the statistic

$$(4) \quad AIC_c = -2 \log_e(\mathcal{L}) + 2\phi \left(1 + \frac{\phi + 1}{n - \phi - 1}\right)$$

where n is the number of data points and ϕ is the number of estimated parameters (including the E_s).

The very large number of possible combinations made examining each potential model formulation impractical; therefore, the model building procedure was conducted in a stepwise fashion. The first step was to establish the simplest form of the model that could reasonably be expected to explain the data: a null hypothesis. The second step identified the S curve that gave the lowest AIC_c value under the null hypothesis. This curve was then used in all subsequent eval-

Table 3. Parameter estimates for the model resulting from the stepwise selection procedure with bootstrap estimates of the coefficient of variation (CV, %), bias (%), and correlation coefficients.

	Estimate	CV	Bias	Correlation coefficients											
				$P_{f,102}$	$P_{s,102}$	$P_{f,126}$	$P_{s,126}$	$P_{f,152}$	$P_{s,152}$	β	α	γ_f	γ_s	θ_1	θ_2
$p_{f,102}$	0.7098	6	0												
$p_{s,102}$	0.9056	15	-1	0.3											
$p_{f,126}$	0.5207	18	-9	0.1	0.0										
$p_{s,126}$	0.6168	26	-9	0.0	0.4	0.6									
$p_{f,152}$	0.3351	25	3	-0.1	-0.1	0.8	0.6								
$p_{s,152}$	0.3658	34	-2	-0.1	0.3	0.5	0.8	0.6							
β	0.9859	1	0	-0.4	-0.2	0.1	0.2	0.3	0.3						
α	1.9000	2	0	0.4	0.2	0.1	0.0	-0.2	-0.1	-1.0					
γ_f	0.0861	5	-3	-0.1	-0.1	0.0	-0.1	0.0	-0.1	0.0	0.0				
γ_s	0.0976	13	-11	0.1	0.0	-0.3	-0.2	-0.3	-0.3	-0.2	0.2	0.1			
θ_1	0.2256	10	0	0.2	0.4	0.0	0.1	0.0	0.0	-0.1	0.1	0.0	-0.1		
θ_2	-0.0398	-10	3	0.0	0.1	0.0	0.0	0.0	0.1	0.0	0.0	0.0	-0.1	-0.3	
θ_3	-0.0024	-37	14	-0.2	-0.3	0.1	0.0	0.1	0.0	0.1	-0.1	0.0	0.1	-0.6	-0.5

Note: The subscripts s and f indicate spring and fall. The bootstrap procedure and bias estimator are discussed in Appendix B.

uations until a final model was selected (at which point the choice of curves was re-evaluated).

The third step proceeded with the goal of identifying the most parsimonious choice of selectivity parameters given the S curve chosen in the previous step and assuming selectivity was invariant among the various k . This was accomplished by adding the parameters to the initial model one at a time and keeping the parameter that gave the lowest AIC_c value. The remaining parameters were then added one at a time to the updated version of the model and the one with the lowest AIC_c score used to update the model further and so on. This procedure was continued until no further improvement in the AIC_c could be obtained. The fourth and final step proceeded similarly, adding seasonal terms to the model that emerged from the third step.

Relationship between encounter rates and abundance

The discussion so far has been framed in terms of S and E rates, but it is changes in abundance that are of most interest to fisheries managers. The local abundance (N) of the population may be derived by dividing the estimates of E by the number of encounters per fish (ϵ)

$$(5) \quad N_{kl} = E_{kl}/\epsilon_{kl}$$

The encounter rate will index N if ϵ is constant, but this seems unlikely because larger fish tend to move about more and are therefore more likely to swim into the net (Lagler 1968).

Random walk and advection-diffusion models indicate that the number of times a fish would be expected to encounter a particular region in space (such as a unit of net) is proportional to its average swimming speed (see, e.g., Okubo 1980), which in turn increases in proportion to l raised to a power (τ) between 0.5 and 1.0 (Beamish 1978; Blake 1983). This suggests

$$(6) \quad \tilde{N}_{kl} = E_{kl}(l/l_\omega)^{-\tau}$$

where \tilde{N} is a measure of relative abundance obtained by dividing N in eq. 5 by the swimming speed at some reference

length l_ω (perhaps the largest length-class defined in the model).

Unfortunately, the exponent τ cannot be estimated from catch and effort data alone, which are conditioned on the number of encounters, and must be determined independently. No such values have been published for red drum; however, Blake (1983) estimated an overall value of 0.8 for the combined observations from a large variety of nonscombrid fish and we suspect red drum will be better represented by this value than by either extreme (0.5 or 1.0). Note that the choice of τ in eq. 6 does not affect the estimates of the selectivity parameters.

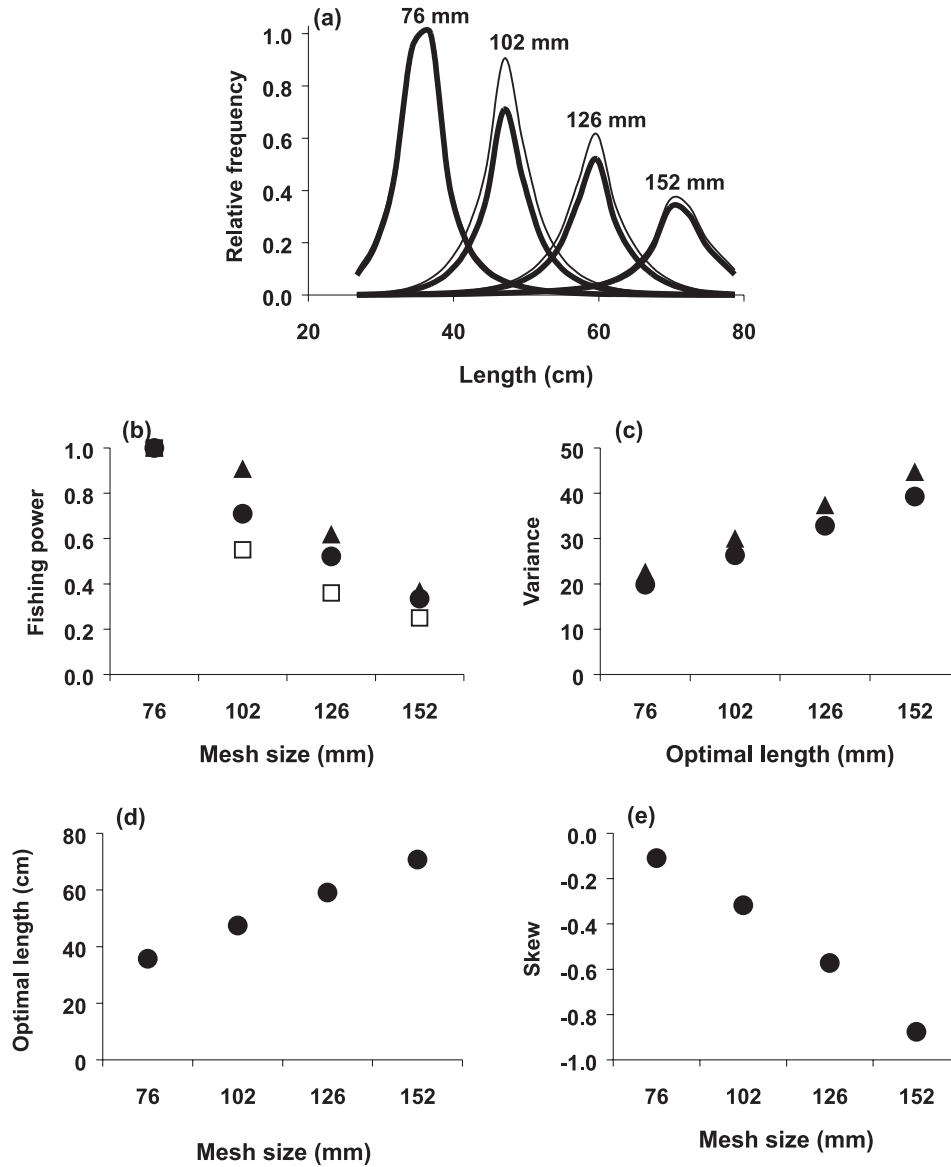
Application to red drum in Texas bays

The Texas Parks and Wildlife Department (TPWD) has used overnight sets of monofilament gillnets to monitor the abundance of red drum and other fish in Texas bays since November of 1975. The nets, composed of four 1.2×45.7 m panels with ms of 76, 102, 127, and 152 mm (stretched), have been deployed in the same way since the program's inception (McEachron and Green 1985; Hensley and Fuls 1998). Over 13 000 sets were made at randomly chosen positions along the shorelines of the nine major bays (Table 2) during two 10-week time periods beginning in the second full week of April (spring) and the second full week of September (fall).

The data were aggregated into strata defined by mesh, bay, season, and fishing year. Fishing years began during the fall, when red drum recruit to the bays, and included the following spring (e.g., the 1976 fishing year includes the fall of 1976 and spring of 1977). Not all of the fish were measured in some sets. Therefore, catch-at-length vectors were obtained by multiplying the relative length-frequency distribution of the measured fish by the total catch of all sets (for a total of 32 676 catch-at-length observations). Effort was measured in terms of the hours each net spent immersed.

Baranov's (1948) similarity principle, which states that S is the same for any given $l:m$ if the quarry grows symmetrically and the primary mode of capture is gilling or wedging, was adopted as the null hypothesis because red drum grow

Fig. 1. Final estimates of (a) selection curves for each mesh size in the spring (thin lines) and fall (thick lines) and (b–e) selectivity parameters from the final model. Circles and triangles represent the estimates corresponding to the fall and spring (where they are different). The squares represent the null hypothesis for the fishing power coefficients.



symmetrically and have few protuberances to encourage tangling. The similarity principle implies a linear relationship between λ and m ($\beta = 1$), constant σ^2 ($\delta = 0$), and no added skew ($\theta = 0$). Initially it was also assumed that p is proportional to the number of potential gilling sites per unit area inasmuch as fish have a tendency to move along the net until they find a place they can pass through or are captured (resulting in fixed relative p values of 1.0, 0.54, 0.33, and 0.23 for the 76-, 102-, 127-, and 152-mm-mesh panels). Subsequently, the statistical contribution of estimating the β , δ , θ , and p terms was evaluated via the model-building procedure discussed earlier. Owing to the consistent manner in which the survey was conducted, the same selection parameters were applied to all years. However, allowance was made for possible differences between the spring and fall, which have very different environmental characteristics.

Coast-wide estimates of \tilde{N} were constructed from the re-

sults of the final model by weighting the bay-specific estimates according to the length of their coastlines (see Hensley and Fuls 1998). Approximate 90% confidence intervals were constructed from the ordered bootstrap results (Appendix B). Sabine lake was not sampled before 1985 (except sparsely in 1975) and East Matagorda bay was not sampled in 1975; however, this should have little impact on the results because both bays together account for only about 7% of the total coastline.

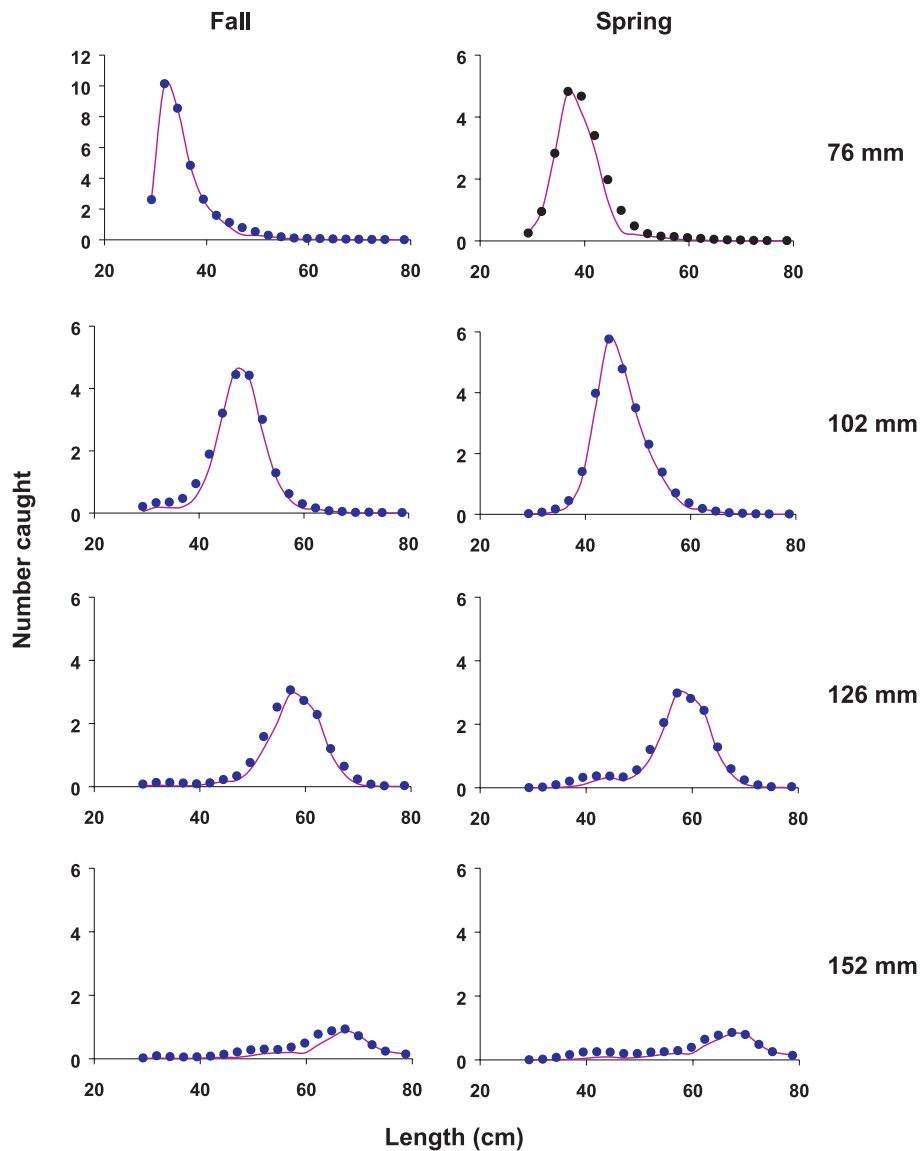
Results

The initial model representing the null hypothesis had only two selection terms (α and γ)

$$(7) \quad C_{mbtyl} = f_{mbty} p_m S\{\lambda = \alpha m, \sigma^2 = \gamma, \theta = 0\} E_{btyl}$$

where the subscripts b , t , and y denote bay, season, and year,

Fig. 2. Model fits (lines) to observed catch-at-length (points) for all bays and years combined.



$p_m = [1.0, 0.54, 0.33, \text{ and } 0.23]$, and S is the unknown selection curve. The final model that emerged from the stepwise procedure added five more selection terms ($\beta, \theta_1, \theta_2, \theta_3$, seasonal γ s) and 6 seasonal p s ($p_{76} = 1.0$),

$$(8) \quad C_{mbtyl} = f_{mbty} p_{mt} S\{\lambda = \alpha m \beta, \sigma^2 = \gamma_i \lambda, \\ \theta = \theta_1 + \theta_2 m + \theta_3 m^2\} E_{btyl}$$

The Laplace distribution was selected to model the shape of S because it gave the lowest AIC_c value for both eqs. 7 and 8.

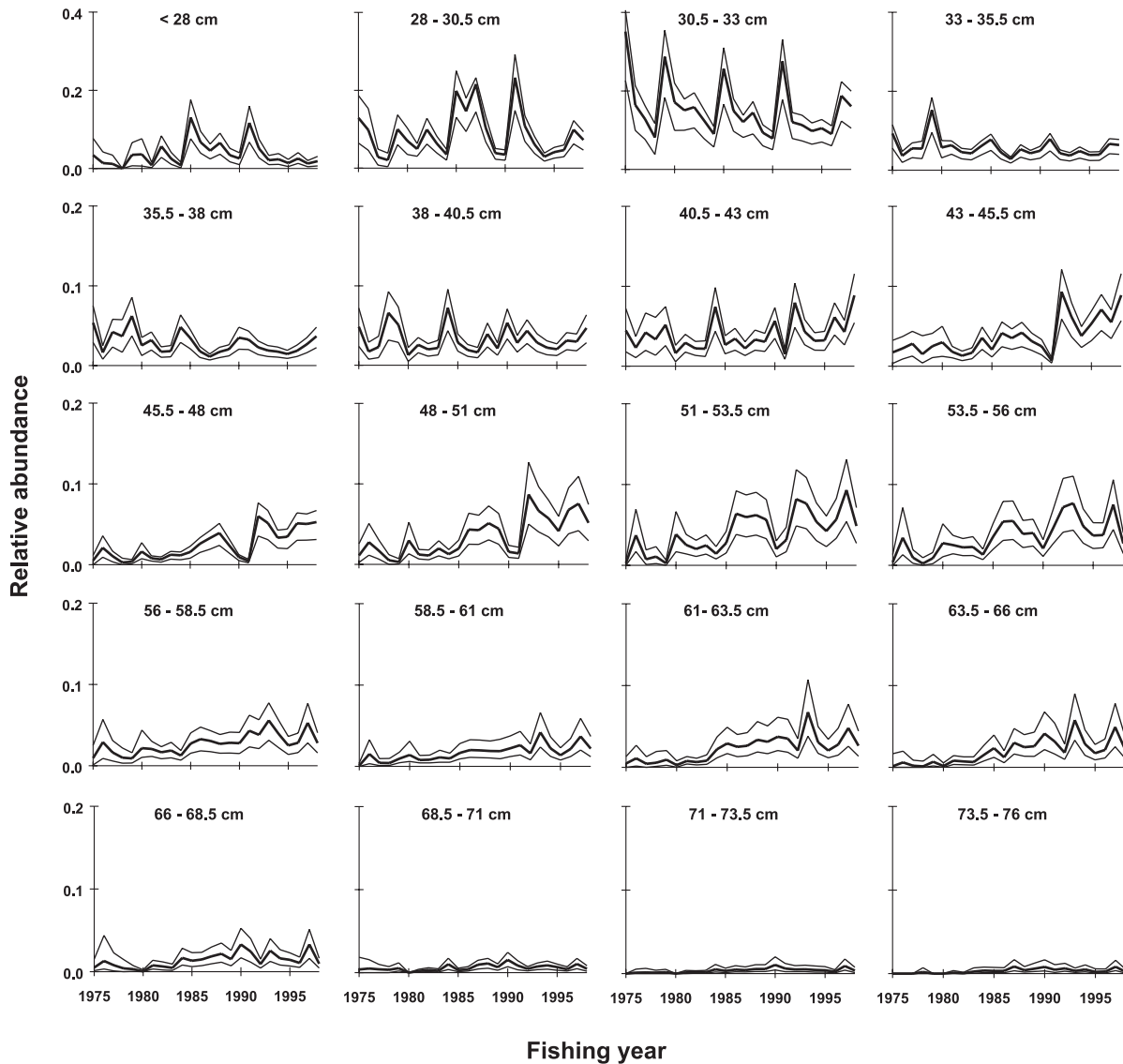
A total of 8434 parameters, including the 8421 E terms, were estimated from 32 676 data points. Nevertheless, the results of the bootstrap procedure indicated that the S and p parameters were well estimated, having low coefficients of variation, negligible bias, and moderate correlations (Table 3). The estimated S curves had the narrow peaks and thick-tailed characteristic of the Laplace distribution and were slightly skewed (Fig. 1a). p was estimated to decrease with m , but less rapidly than postulated by the null hypothesis (Fig. 1b). λ increased almost linearly with m as hypothe-

sized (Fig. 1c), the estimated exponents (β) being close to, but statistically different from, 1.0. The σ^2 was not constant, as originally hypothesized, but increased linearly with λ (Fig. 1d). The estimates for the skew parameters ($\theta_1, \theta_2, \theta_3$) were significantly different from 0 and suggest increasingly negative skew with m (Fig. 1e). The variance and fishing power coefficients were significantly higher in the spring than in the fall, but no significant seasonal effects were found for the optimal length and skew parameters.

The model provided a good overall fit to the catch data (Fig. 2), but the predictions along the tails of the distributions tended to be somewhat lower than the observed values. This pattern is largely due to the proportionally higher variances associated with the low catch rates in the tails and was much less conspicuous when each catch observation was weighted equally. In any case, the estimates of abundance were similar for the variance-weighted and equally weighted fitting procedures, suggesting that they are robust with respect to the model's ability to fit the tails.

The coast-wide estimates of abundance fluctuate markedly

Fig. 3. Estimated relative abundance of red drum (*Sciaenops ocellatus*) in Texas bays during the fall (heavy centerline) with 90% confidence intervals (thin lines).



despite having narrow confidence intervals (Figs. 3 and 4), indicating that the recruitment and survival of red drum in Texas bays is highly variable. The estimates for fish under 40.5 cm in length exhibit no discernible long-term trends; however, the estimates for larger fish show a strong increasing trend during the 1980s and 1990s. Age-length data from otoliths collected during the 1990s (Fig. 5) indicate that red drum less than 40.5 cm long in the fall and 46 cm in the spring are nearly all one year old and that red drum less than 53.5 cm long in the fall and 58.5 cm in the spring are nearly all two years old. Most of the remaining catch is composed of fish between three and four years old.

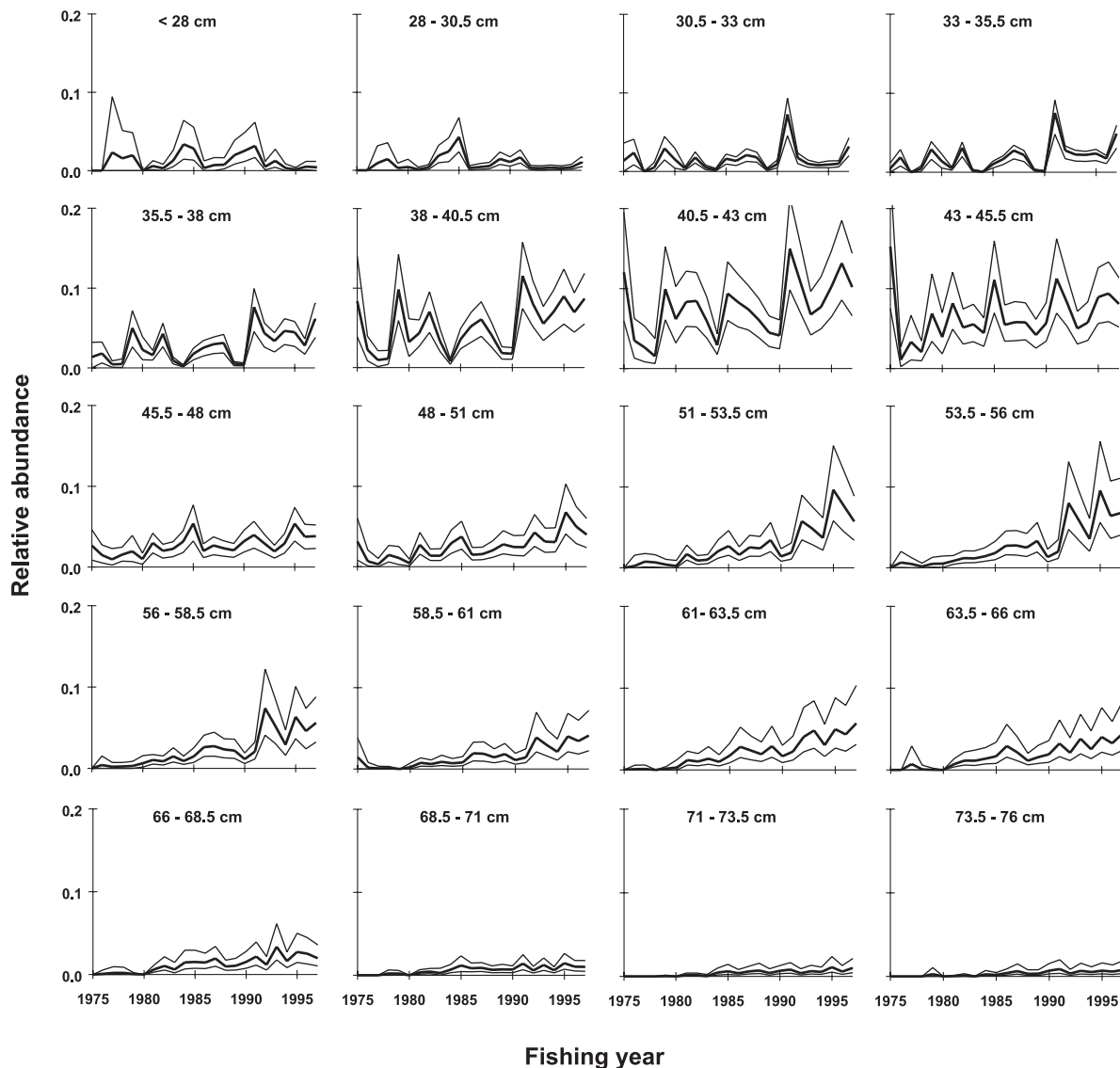
Approximate indices of survival were developed by aggregating the length distributions according to age and dividing the estimated abundance of each year-class by its estimated abundance during the preceding year (Fig. 6). The results suggest the survival of age-1 red drum has increased steadily from very low values in the 1975 to nearly 100% by the late 1990s. The survival of age-2 red drum also seems to have in-

creased since 1975, but leveled off during the mid-1980s and began fluctuating between 50% and 100%. The survival of age-3 and older fish remained very low.

Discussion

The selection models presented in this paper accommodate the possibility that some catch-at-length observations will be known more precisely than others and allow for non-linear relationships between the optimal length, variance in length, and mesh size. The example showed that gillnet selection for red drum in Texas bays could be explained as a unimodal process approximating a skewed Laplace distribution where the optimal length varies in proportion to mesh size and the variance in proportion to the optimal length (therefore also proportional to mesh size). The proportional relationship between optimal length and mesh size is not surprising and has been demonstrated for many species (see Hamley 1975). The proportional relationship between vari-

Fig. 4. Estimated relative abundance of red drum (*Sciaenops ocellatus*) in Texas bays during the spring (heavy center line) with 90% confidence intervals (thin lines).



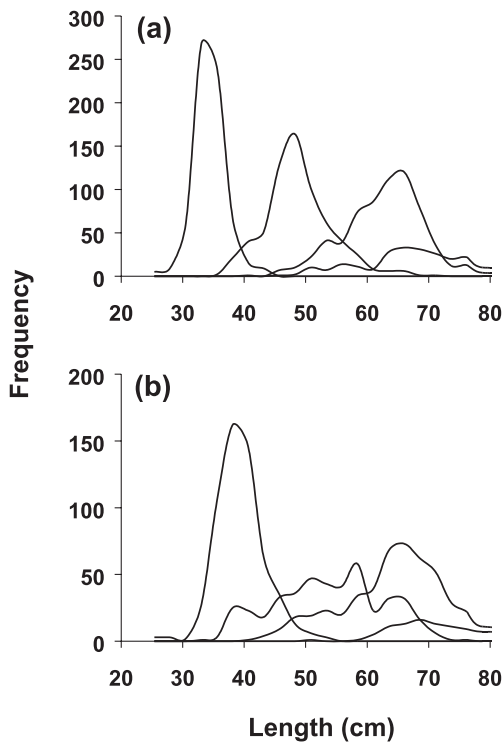
ance and mesh size, on the other hand, is intermediate between the usual assumptions of either constant variance or variance proportional to the square of mesh size. In fact, the “usual” assumptions likely represent the extremes of the relationship and we suggest that allowance always be made for linear forms.

The estimated fishing power for red drum was greater for the spring than for the fall, probably owing to an increase in swimming activity associated with the warmer spring temperatures (see Hensley and Fuls 1998). The estimates also decreased with mesh size, but not as rapidly as the decrease in capture sites per unit of net. This suggests that larger fish may be channeled into the large mesh panels by the adjacent smaller mesh panels or that larger fish cover a greater area of net with each encounter. In any case, the decreasing trend would seem counter to the conventional wisdom that larger meshes are more efficient (Hamley 1975). The conventional wisdom, however, is largely based on fishing power coefficients

derived from direct comparisons of gillnet catches with known populations, which implicitly reflect the potential increase in encounter rates with length. When the power estimates from this study were multiplied by the relative encounter rates for the corresponding optimal lengths (with $\tau = 0.8$), the values did indeed increase with mesh size.

The fishing power of gillnets usually decreases as fish and debris accumulate in them (Hamley 1975), causing the catch rates to level off and making the population seem more stable than it actually is (hyperstability). On the other hand, if the target species is attracted by an increase in certain of the entangled items their catch rate may accelerate, causing trends in the population to appear stronger than they actually are (hyperdepletion). If the target species is the predominant item caught, this effect could be estimated by parameterizing fishing power as $p = gE^h$ (and suitably modifying eq. 3), where $h < 1$ would indicate hyperstability and $h > 1$ hyperdepletion (g is a scaling coefficient). Otherwise, it may be

Fig. 5. Distributions of length for ages 1, 2, 3, and 4 during the (a) fall and (b) spring.



more appropriate to express p as a function of some other covariate like the total number of items entangled. Neither approach appears necessary for the present example as the catch per hour of red drum was not significantly correlated with soak time. Moreover, net saturation was not a frequent problem; less than one percent of the gilling sites were occupied in most sets and less than five percent of the gilling sites were occupied in 99% of the sets. Red drum themselves constituted only a small fraction of the total catch.

The fall abundance of red drum under 40 cm in length (presumably age 1) was estimated to fluctuate without a persistent trend. In part, this appears to be a reflection of recruitment inasmuch as the catch rate of young-of-the-year (age-0) red drum in bag seines also fluctuates with little trending (Hensley and Fuls 1998). However, the age-0 bag seine and lagged age-1 gillnet series are not highly correlated, implying that the survival of age-0 red drum is also highly variable. This contention is supported by observations of increased survival associated with hurricanes (Matlock 1987) and catastrophic kills associated with severe cold fronts (McEachron et al. 1994).

In contrast to fish under 40 cm in length, the abundance and survival of larger red drum appears to have increased a great deal since the early 1980s. This is consistent with increasingly restrictive regulatory changes promulgated by the state of Texas during the 1980s, starting in 1981 when the commercial sale of red drum was prohibited, the minimum length limit was increased from 35.6 to 40.6 cm, and the maximum length limit was lowered to 76.2 cm. In 1988 the minimum length limit was increased to 50.8 cm, the maximum length limit reduced to 71.1 cm, and a creel limit of 3 fish per day was imposed. These regulations effectively

eliminated most of the fishing pressure on age-1 and -2 red drum, which is reflected by the very high survival rates indicated in this study.

The fraction of age-3 red drum remaining in the study area was estimated to be very low with little indication of an increasing trend, but the exact magnitude is hard to determine owing to the difficulty in distinguishing age-3 and -4 red drum based on length. To a large extent, the low values may be a reflection of the emigration of maturing 3- and 4-year-old fish out of the bays and into offshore waters, which probably exceeds the loss rate due to fishing and makes any increase in survival difficult to detect. The prohibition on commercial harvest in 1981 and subsequent creel limits may have resulted in a slight increase in spring-to-spring survival of age-3 red drum, but their effect seems to have been mitigated by a shift in recreational effort away from smaller fish (anglers being forced to fill their creel limits with fish within the size limits, most of which are age 3 and 4).

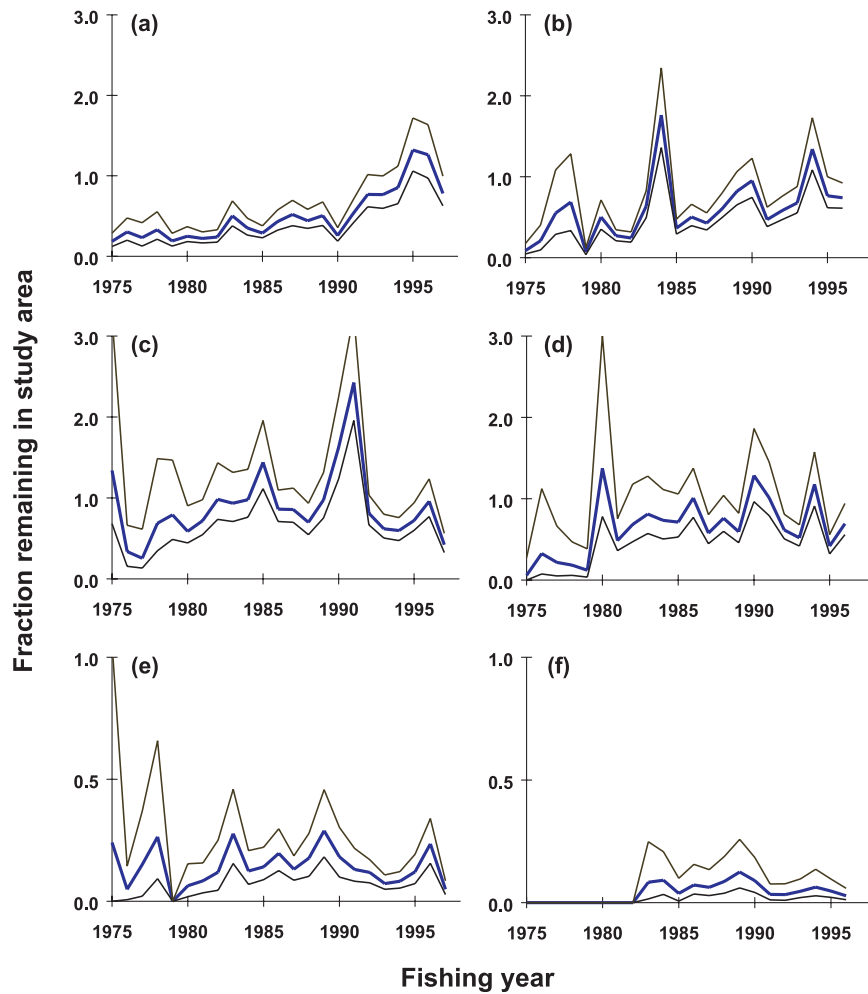
It is noteworthy that the lower confidence limit of the fraction of red drum remaining in the study area occasionally exceeds 1.0, which suggests there may sometimes be a net influx of fish into the study area. This is likely a consequence of episodic movements such as might occur with the passage of cold fronts when red drum are temporarily driven out of the shallow near-shore areas into the deeper waters of the bays. Such variations, however, are effectively random over the time scale considered here and should not affect the long-term trends.

Texas bay systems have experienced a net loss of emergent wetlands and submerged aquatic vegetation since 1975 owing to subsidence, erosion, upland conversion, and dredge-and-fill activities (Galveston Bay National Estuary Program 1995; Texas Parks and Wildlife Department 1999). This raises concerns that the spatial distribution of red drum has changed through time, with a larger fraction concentrating along the remaining healthy shorelines or perhaps using parts of the bay further away from the shore. The former response should not bias the estimated survival and abundance trends because the sampling procedure has not changed, i.e., stations located in the damaged areas are still sampled in the same way. The latter response, however, could lead to a negative bias in the estimated trends because a decreasing fraction of the total population would be available to the nets. However, this too seems unlikely because red drum do not appear to use the open portions of the bay; trawl surveys conducted in these areas by the TPWD have rarely caught red drum and there has not been a discernible increase since the survey began in 1982.

One could argue that the abundance and survival indices may be sensitive to the value of the exponent τ used in the speed-to-length relationship, which was not estimable from the types of data examined in this study and had to be borrowed from a meta-analysis by Blake (1983). However, the rate of increase in abundance was only slightly depressed when the extreme value of 1.0 was used for τ instead of 0.8. Thus, explicit consideration of the uncertainty in τ , if it were possible, would broaden the confidence intervals somewhat, but the general conclusions would remain unchanged.

A reviewer also suggested that a multiplicative error structure might be more appropriate than the weighted least-

Fig. 6. Fraction of red drum in each age-class that remain in the study area after one year (from one fall to the next or one spring to the next) with 90% bootstrap confidence intervals. Panels (a) and (b) refer to the fraction of age-1 fish remaining at age 2. Panels (c) and (d) refer to the fraction of age-2 fish remaining at age 3. Panels (e) and (f) refer to the fraction of age-3 fish remaining at age 4.



squares approach adopted here, in which case the task would be to minimize

$$(9) \quad \mathcal{L} = \sum_l \sum_k \sum_m (\log_e \{C_{mkl} + z\} - \log_e \{f_{mk} p_{mk} S_{mkl} E_{kl} + z\})^2$$

The small constant z must be added to each observation if there are catches of zero (as there are in the present example), whereupon the computational burden is greatly increased because there is no closed-form solution for the E terms. Moreover, eq. 9 implies that the variance of C increases in proportion to the squared expectation of C , whereas our data suggest a more linear relationship. For these reasons, a better alternative for the present example might be a Poisson error structure, where one seeks to minimize

$$(10) \quad \mathcal{L} = \sum_l \sum_k \sum_m f_{mk} p_{mk} S_{mkl} E_{kl} - C_{mkl} \log_e \{f_{mk} p_{mk} S_{mkl} E_{kl}\}$$

where

$$E_{kl} = \frac{\sum_m C_{mkl}}{\sum_m f_{mk} p_{mk} S_{mkl}}$$

Note, however, that neither eqs. 9 or 10 allow the variance of C to vary with the number of sets, which are few during the early part of the time series for red drum.

We applied the Poisson error structure to the final selection model in eq. 8 and found that the fishing power estimates for 102- and 126-mm mesh were between 15 and 35% lower than the corresponding weighted least-squares estimates. This translated into proportionally higher abundance estimates for ages 2 and 3 (relative to age 1), which in turn suggested somewhat higher survival rates from age 1 to age 2. Otherwise, the abundance and survival trends were nearly identical to those estimated by the weighted least-squares approach.

Acknowledgments

This paper is dedicated to the memory of Larry McEachron, who succumbed to cancer before the review

process was completed. We thank Carl Walters and two anonymous reviewers for their helpful comments on the manuscript and the Texas Parks and Wildlife Department for releasing the data. Partial funding for the data collection was provided by the U.S. Department of Interior, Fish and Wildlife Service (DJ 15.605, Project F-34-M).

References

- Baranov, F.I. 1948. Theory and assessment of fishing gear. Pishchepromizdat, Moscow.
- Beamish, F.W.H. 1978. Swimming capacity. *In* Fish physiology. Vol. 7. Locomotion. *Edited by* W.S. Hoar and D.J. Randall. Academic Press, New York. pp. 101–187.
- Blake, R.W. 1983. Fish locomotion. Cambridge University Press, New York.
- Buckland, S.T., Burnham, K.P., and Augustin, N.H. 1997. Model selection: an integral part of inference. *Biometrics*, **53**: 603–618.
- Croxtan, F.E., Cowden, D.J., and Klein, S. 1967. Applied general statistics. 3rd ed. Prentice Hall, Englewood Cliffs, N.J.
- Efron, B. 1992. Six questions raised by the bootstrap. *In* Exploring the limits of bootstrap. *Edited by* R. LePage and L. Billard. John Wiley and Sons, New York.
- Fournier, D.A., Sibert, J.R., Majkowski, J., and Hampton, J. 1990. MULTIFAN a likelihood-based method for estimating growth parameters and age composition from multiple length frequency data sets illustrated using data for southern bluefin tuna (*Thunnus maccoyi*). *Can. J. Fish. Aquat. Sci.* **47**: 301–317.
- Galveston Bay National Estuary Program. 1995. The Galveston Bay Plan. Publication GBNEP-49. Galveston Bay National Estuary Program, Webster, Texas.
- Hamley, J.M. 1975. Review of gillnet selectivity. *J. Fish. Res. Board Can.* **32**: 1943–1969.
- Hamley, J.M., and Regier, H.A. 1973. Direct estimates of gillnet selectivity to walleye (*Stizostedion vitreum vitreum*). *J. Fish. Res. Board Can.* **30**: 817–830.
- Helsler, T.E., Condrey, R.E., and Geaghan, J.P. 1991. A new method of estimating gillnet selectivity, with an example for spotted seatrout, *Cynoscion nebulosus*. *Can. J. Fish. Aquat. Sci.* **48**: 487–492.
- Hensley, R.A., and Fuls, B.E. 1998. Trends in relative abundance and size of selected finfishes and shellfishes along the Texas coast: November 1975 – December 1996. Texas Parks and Wildlife Department Management Data Series Number 159, 4200 Smith School Road, Austin, TX 78744, U.S.A.
- Holt, S.J. 1963. A method of determining gear selectivity and its application. ICNAF–ICES–FAO Joint Sci. Meet. Pap. No. S15 (ICNAF Spec. Publ. No. 5. pp. 106–115).
- Hovgard, H. 1996. A two-step approach to estimating selectivity and fishing power of research gill nets used in Greenland waters. *Can. J. Fish. Aquat. Sci.* **53**: 1007–1013.
- Hurvich, C.M., and Tsai, C. 1995. Model selection for extended quasi-likelihood models in small samples. *Biometrics*, **51**: 1077–1084.
- Lagler, K.F. 1968. Capture, sampling and examination of fishes. *In* Methods for assessment of fish production in fresh waters. IBP Handbook 3. *Edited by* W.E. Ricker. Blackwell Scientific Publications, Oxford. pp. 7–45.
- Matlock, G.C. 1987. The role of hurricanes in determining year-class strength of red drum. *Contrib. Mar. Sci.* **30**: 39–47.
- McCombie, A.M., and Berst, A.H. 1969. Some effects of shape and structure of fish on selectivity of gill nets. *J. Fish. Res. Board Can.* **26**: 2681–2689.
- McCombie, A.M., and Fry, F.E. 1960. Selectivity of gill nets for lake whitefish, *Coregonus clupeaformis*. *Trans. Am. Fish. Soc.* **89**: 176–184.
- McEachron, L.W., and Green, A.W. 1985. Trends in relative abundance and size of selected finfish in Texas bays: November 1975 – June 1984. Texas Parks and Wildlife Department Management Data Series Number 79. Texas Parks and Wildlife Department, 4200 Smith School Road, Austin, TX 78744, U.S.A.
- McEachron, L.W., Matlock, G.C., Bryan, C.E., Unger, P., Cody, T., and Martin, J.H. 1994. Winter mass mortality of animals in Texas Bays. *Northeast Gulf Sci.* **13**: 121–128.
- Okubo, A. 1980. Diffusion and ecological problems: mathematical models. Springer-Verlag, New York.
- Porch, C.E. 1998. Some intrinsic limitations of sample variances in stock assessment models. *In* Fishery stock assessment models. *Edited by* F. Funk, T.J. Quinn, II, J. Heifetz, J.N. Ianelli, J.E. Powers, J.F. Schweigert, P.J. Sullivan, and C.-I. Zhang. Alaska Sea Grant College Program Report No. AK-SG-98-01. University of Alaska, Fairbanks. pp. 385–398.
- Regier, H.A., and Robson, D.S. 1966. Selectivity of gill nets, especially to lake whitefish. *J. Fish. Res. Board Can.* **23**: 423–454.
- Scheaffer, R.L., Mendenhall, W., and Ott, L. 1979. Elementary survey sampling. 2nd ed. Duxbury Press, North Scituate, Mass.
- Seber, G.A.F., and Wild, C.J. 1989. Nonlinear regression. John Wiley and Sons, New York.
- Texas Parks and Wildlife Department. 1999. Seagrass conservation plan for Texas. Texas Parks and Wildlife Department, Austin.

Appendix A. Derivation of variance formulae

The catch-at-length observations for each mesh–strata combination, C_{mkl} , were the product of the observed total catch from the mesh (T_{mk}) and the proportion of that catch that belonged to a particular length category (x_{mkl}). We assume the covariance between T and x is small within any given k , in which case the variance of C_{mkl} is

$$V\{C_{mkl}\} \approx T_{mk}^2 V\{p_{mkl}\} + x_{mkl}^2 V\{T_{mk}\}$$

A substantial covariance between T and x might occur if each mesh catches members of several year-classes and year-class strength varies considerably through time—high T values would tend to be associated with high x values for the length categories corresponding to the strong year-class. We do not expect this to be a significant problem in our analysis of Texas red drum because each mesh size catches fish that are predominantly from one age-class (owing to the rapid growth rate of red drum), and year-class strengths do not appear to vary greatly from one year to the next (Hensley and Fuls 1998).

Variance of total catch T

The catches of each individual set i of mesh m in any given k (c_{imk}) can be treated as statistically independent because the sets were separated in time and space and the catches were negligible compared with the local population abundance. If the c_{imk} were also identically distributed, an unbiased estimate of the variance of the total catch T_{mk} by all sets would be

$$V\{T_{mk}\} \approx \frac{n_{mk}}{n_{mk} - 1} \sum_i (c_{imk} - \sum_i c_{imk} / n_{mk})^2$$

where n_{mk} is the number of sets with mesh m in strata k . However, in this case, the c_{imk} were not identically distributed because the soak time f_{imk} was not the same for all sets. This being the case, we note that the total catch T_{mk} is simply the product of the total effort and the ratio estimator for the expected catch per unit effort

$$\widehat{R}_{mk} = \frac{\sum_i^{n_{mk}} c_{imk}}{\sum_i^{n_{mk}} f_{imk}}$$

The soak time of each set was independent of the catch rate; therefore

$$V\{T_{mk}\} = \left(\sum_i f_{imk}\right)^2 V\{\widehat{R}_{mk}\} + \widehat{R}_{mk}^2 V\left\{\sum_i f_{imk}\right\}$$

where $V(\sum_i f_{imk})$ is replaced by the equivalent sample statistic and $V(\widehat{R}_{mk})$ is given by Scheaffer et al. (1979) as

$$V\{\widehat{R}_{mk}\} = \frac{1}{n_{mk} \bar{f}_{mk}^2} \frac{\sum_i (c_{imk} - \widehat{R}_{mk} f_{imk})^2}{n_{mk} - 1}$$

Variance of the proportion x in each length-class

The observations of length for each mesh and stratum are essentially random samples from the vulnerable fraction of the population. The proportion of the catch falling in each length-class, x_{mkl} , is therefore a random variable with mean μ , sample size v , and variance $(1 - \mu)\mu/v$. As such, Fournier et al. (1990) advocate using the formula

$$V\{p_{mkl}\} = \frac{(1 - \hat{x}_{mkl})\hat{x}_{mkl} + 0.1/L}{v_{imk}}$$

where the μ are replaced by the model estimates (\hat{x}_{mkl}) and L is the number of length categories. The term $0.1/L$ is included to prevent the expression from tending to zero as x tends to zero.

Replacing the μ with the model estimates presents a problem in the present case because the E s in eq. (3) can no longer be solved for analytically. This leaves us in the unenviable position of having to solve for thousands of pa-

rameters numerically. To avoid this we use the perhaps less satisfactory approach of replacing the model estimates with the observed values pooled over all sets within a given stratum. This may cause anomalously low observations of catch-at-length to receive too much weight in the analysis (see Porch 1998), but the effect should not be too serious because a large number of observations are made within each stratum so that the pooled length-frequency distributions should be a fairly good reflection of the true distribution. Moreover, the use of observed values should render the results less sensitive to model mis-specification. Regardless, we believe it to be superior to simply assuming that the variances of all observations are identical.

Appendix B. Bootstrap estimates of variance and bias of parameters

The bias of a statistic $\hat{\theta}(\text{C})$ as an estimate of a given quantity θ was computed as

$$\text{bias}\{\hat{\theta}(\text{C})\} = \frac{1}{500} \sum_{B=1}^{500} \hat{\theta}(\text{C}^B) - \hat{\theta}(\sum \text{C}^B / B)$$

where C is the matrix of observed catches at length (original data), C^B is a matrix of bootstrapped catches at length, and B is one of 500 bootstrap replications (Efron 1992). Approximate confidence limits were constructed by ordering the results of each bootstrap (the percentile method).

Each bootstrap data set C^B was generated parametrically

$$\begin{aligned} \text{C}_{mkl}^B &= T_{mk}^B x_{mkl}^B \\ T_{mk}^B &= \hat{T}_{mk}(\text{C}) + \eta^B \end{aligned}$$

Here, $\hat{T}_{mk}(\text{C})$ is the expected value of total catch obtained when the model was applied to the original data and η^B represents a random draw from the normal distribution with mean 0 and variance equal to the observed sample variance $V\{T_{mk}\}$. The variable x_{mkl}^B represents the bootstrap relative frequency distribution of length generated by drawing with replacement from the corresponding model-estimated relative length-frequency distribution, $\hat{x}_{mkl}(\text{C})$. The number of draws from $\hat{x}_{mkl}(\text{C})$ was the lesser of the actual number measured (v_{mk}) or T_{mk}^B .